ACS APPLIED MATERIALS & INTERFACES

Research Article

www.acsami.org

Facile Preparation of Core–Shell Magnetic Metal–Organic Framework Nanoparticles for the Selective Capture of Phosphopeptides

Yajing Chen, Zhichao Xiong, Li Peng, Yangyang Gan, Yiman Zhao, Jie Shen, Junhong Qian, Lingyi Zhang, and Weibing Zhang*

Shanghai Key Laboratory of Functional Materials Chemistry, Department of Chemistry and Molecular Engineering, East China University of Science and Technology, Shanghai 200237, China

Supporting Information

ABSTRACT: In regard to the phosphoproteome, highly specific and efficient capture of heteroideous kinds of phosphopeptides from intricate biological sample attaches great significance to comprehensive and in-depth phosphorylated proteomics research. However, until now, it has been a challenge. In this study, a new-fashioned porous immobilized metal ion affinity chromatography (IMAC) material was designed and fabricated to promote the selectivity and detection limit for phosphopeptides by covering a metal–organic frameworks (MOFs) shell onto Fe_3O_4 nanoparticles, taking advantage of layer-by-layer method (the synthesized nanoparticle denoted as Fe_3O_4@MIL-100 (Fe)). The thick layer renders the nanoparticles with perfect hydrophilic character, super large surface area, large immobilization of the Fe^{3+} ions and the special porous structure. Specifically, the as-synthesized MOF-decorated magnetic nanoparticles own an ultra large surface area which is up to 168.66 $m^2\ g^{-1}$ as well as two appropriate pore sizes of 1.93 and 3.91 nm with a narrow grain-size distribution and rapid separation under the magnetic circumstance. The unique features vested the synthesized nanoparticles an excellent ability for phosphopeptides enrichment with high selectivity for β-casein (molar ratio of β-casein/BSA, 1:500), large enrichment capacity (60 mg g^{-1}), low detection limit (0.5 fmol), excellent phosphopeptides recovery (above 84.47%), fine size-exclusion of high molecular weight proteins, good reusability, and desirable batch-to-batch repeatability. Furthermore, encouraged by the experimental results, we successfully performed the as-prepared porous IMAC nanoparticle in the specific capture of phosphopeptides from the human serum (both the healthy and unhealthy) and nonfat milk, which proves itself to be a good candidate for the enrichment and detection of the low-abundant phosphopeptides from complicated biological samples.

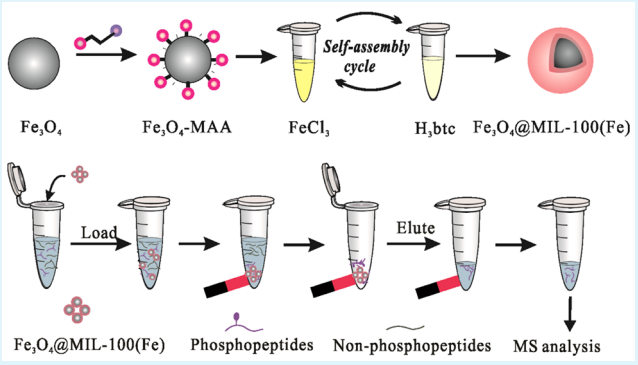

KEYWORDS: *magnetic nanoparticles, metal–organic framework (MOF), phosphorylated peptides, mass spectrum, size-exclusion*

1. INTRODUCTION

Reversible protein phosphorylation, as one of the most vital and ubiquitous post-translational modifications for proteins, plays a significant place in controlling many intricate bioprocesses, such as cellular growth and division, metabolic pathways, and signaling transduction.[1,2] As it is estimated, nearly 30% of all proteins in a cell are at a phosphorylated state at any certain time,[3] so research into the phosphorylation mechanism is of great interest in the proteomics fields. For the sake of better understanding these biological processes, the accurate qualification and quantification of the targeted phosphorylated proteins is a precondition. Currently, mass-spectrometric techniques have been widely considered to be the preferred technology for the characterization of phosphorylation due to its wide dynamic range, ultra high sensitivity, and rapid analytical speed. However, low dynamic stoichiometry and severe signal interference resulted from the high abundance of their native counterparts make mass spectrometry (MS) analysis of phosphopeptides without pretreatment still a challenge. Thus, an effective capture and enrichment for phosphopeptides from complicated biological sample in advance of MS analysis is indispensible.

Until now, several methods and materials embracing immune affinity capture (IAC),[4] metal oxide affinity chromatography (MOAC),[5−7] immobilized metal ion affinity chromatography (IMAC),[8−11] and ion exchange chromatography (IEC)[12,13] have been developed to the sample pretreatment in phosphoproteome. Among the above-mentioned approaches, immobilized metal ion affinity chromatography (IMAC), relying on the interactions among the target analytes and

Received: April 17, 2015
Accepted: July 9, 2015
Published: July 9, 2015

DOI: 10.1021/acsami.5b03335
ACS Appl. Mater. Interfaces 2015, 7, 16338−16347

metal ions fixed on the support material, is utilized most widely. And a series of IMAC materials with different matrixes (e.g., silica, polymer, magnetic nanoparticle, mesoporous bead) were applied in phosphopeptides enrichment. Qian et al.[14] fabricated a kind of Fe^{3+}-immobilized magnetic nanoparticles (Fe^{3+}-IMAN), which was successfully applied in the identification of a large number of phosphorylation sites in plasma membranes from the mouse liver. Feng et al.[15] developed a new method to prepare Fe^{3+}-immobilized metal affinity chromatography monolithic column, showing great prospect for the phosphoproteome analysis. In recent years, porous IMAC materials have been widely applied in phosphopeptides researches due to its good traits of super large surface area, unique pore volume, and regular porous structure. Pan et al.[16] presented a Fe^{3+}-decorated mesoporous nanoparticles of MCM-41. After enrichment, large amounts of nonphosphopeptides from tryptic digest were effectively wiped out, and the MS signal of phosphopeptides was sharply improved. Despite these successful cases, the design and facial preparation of a porous IMAC material with high functional sites and easy separation ability so as to enhance the phosphopeptides capture efficiency is still a highly desirable concern.

As for the orthodox IMAC techniques, centrifugation at high speed during the separation period is usually required, which inevitably results in a cumbersome pretreatment process and unnecessary loss of the target phosphopeptides. As an alternative technology, the magnetic-based matrix has gained immense interest because of the quick response of magnetic beads under magnetic fields. The functionalized magnetic nanoparticles have been widely used in proteomic studies in recent years.[17,18] For phosphopeptide enrichment, a variety of magnetic IMAC nanoparticles were designed and synthesized recently,[19,20] they showed good selectivity and high efficiency. And the porous magnetic IMAC materials own the traits of the porous materials with high surface area that could help to offer more functional sites on the material and further boost the enrichment efficiency. Lu et al.[21] prepared magnetic mesoporous titania microspheres that have super large surface area, unique porous structure with narrow size distribution, and excellent magnetic responsiveness under magnetic field and exhibit high specificity and exceptional enrichment capacity toward phosphopeptides. Hence, the design and preparation of original magnetic porous IMAC materials for higher enrichment efficiency has still been a research hotspot until now.

Metal−organic frameworks (MOFs), also called as porous coordination polymers, which are famous for their super high porosity and incredibly large inner surface areas, have been extensively employed in storage,[22] separation,[23−26] sensing[27] and drug delivery.[28] Because MOFs have abundant surface modifications and porous character, increasing attention has been paid to their application in proteomic research.[29−33] Besides, the perfect pore size also affiliates the material with the size-exclusion effect, which can be used to selectively capture the low molecular weight biomolecules and simultaneous exclude the high molecular weight proteins in complex biological samples.[34−36] However, MOFs-decorated magnetic nanoparticle has rarely been reported in phosphopeptides enrichment. Deng et al.[37] prepared hydrophilic magnetic microspheres modified with zirconium-based MOFs, which presented a high selectivity and recovery for phosphopeptides enrichment. The MOF layer perfectly integrates the brilliant features of Fe_3O_4 and dopamine, greatly improving the hydrophilic character as well as the density of the metal ions of the material. Thus, the synthesis of MOFs-coated magnetic nanospheres by a simple and valid approach for phosphopeptides enrichment would be of great interest to the proteomic fields.

Herein, a new porous IMAC material, the Fe_3O_4@MIL-100 (Fe) nanospheres, has been developed and prepared by means of a facial and dependable layer-by-layer assembly method to selectively enrich the phosphopeptides. The porous structure and the large amount of coordinated Fe (III) endow the magnetic nanoparticles with numerous functional spots for large enrichment capacity and excellent selectivity for phosphopeptides and the perfect size-exclusion effect for high molecular weight proteins. In addition, the magnetic character will promote the quick and total separation of the material. The enrichment efficiency of the IMAC nanoparticles in phosphopeptides enrichment has been examined by applying them in different mimic biological samples. What's more, the practical applicability of Fe_3O_4@MIL-100 (Fe) nanoparticles was investigated by capturing the trace phosphopeptides in tryptic digest of nonfat milk and human serum samples. The specific selectivity, low detection limit, excellent enrichment recovery, large binding capacity and unique size-exclusion effect of the Fe_3O_4@MIL-100 (Fe) nanoparticles for phosphopeptides clearly present them as good adsorbent for phosphoproteome research.

2. EXPERIMENT SECTION

2.1. Reagents and Chemicals. Iron chloride hexahydrate ($FeCl_3·6H_2O$), anhydrous ethanol, ethylene glycol (EG), 1,4-benzenedicarboxylic acid (BDC), *N*,*N*-dimethylformamide (DMF), chloroform and anhydrous sodium acetate (NaAc) were purchased from Tianjin Chemical Plant (Tianjin, China). *β*-casein, *α*-casein (from bovine milk), and bovine serum albumin (BSA), 2,5-dihydroxybenzoic acid (DHB), sinapinic acid (SA), dithiothreitol (DTT), iodoacetamide (IAA), trypsin (TPCK treated), benzene-1,3,5-tricarboxylic acid (H_3btc), mercaptoacetic acid (MAA) and concentrated ammonia aqueous solution ($NH_3·H_2O$, 28−30 wt %) were obtained from Sigma-Aldrich (St. Louis, MO). Trifluoroacetic acid (TFA), HPLC grade acetonitrile (ACN), zirconium chloride ($ZrCl_4$) and ammonium bicarbonate (NH_4HCO_3) were purchased from Aladdin (Shanghai, China). Nonfat milk was bought from a local shop. Healthy human serum was afforded by a volunteer from Dalian Medical University, and unhealthy human serum from an endometrial cancer patient was offered by Fudan University Shanghai Cancer Center. The human serum was stored at −80 °C for further treatment. The standard phosphopeptide (LRRApSLGGK) was bought from Shanghai Apeptide Co., Ltd., (Shanghai, China). The chemicals above were utilized without any treatment. Water was purified by a Milli-Q apparatus (Millipore, Bedford, MA).

2.2. Fabrication of Fe_3O_4@MIL-100 (Fe) Core−Shell Magnetic Nanoparticles. The Fe_3O_4 nanospheres were synthesized by means of a modified solvothermal approach. Specifically, 1.35 g of $FeCl_3·6H_2O$ was dissolved in 75 mL of EG under ultrasonation with an addition of 3.6 g of NaAC. After being vigorously stirred for half an hour, the mixture was shifted to a Teflon-lined stainless steel autoclave, kept under 200 °C for 16 h and collected with natural cooling to room temperature. Then, 350 mg of the above-synthesized Fe_3O_4 nanoparticles were washed with ethanol three times and added to 75 mL of ethanol containing 0.58 mM of MAA, which was gently stirred under nitrogen protection for 24 h. The resulting product (denoted as Fe_3O_4-MAA) was collected with a magnet, washed with ethanol several times until there was no pungent smell and then redispersed in ethanol. A versatile step-by-step assembly strategy was utilized to fabricate the porous Fe_3O_4@MIL-100 (Fe) core−shell nanoparticles. Briefly, 100 mg of Fe_3O_4-MAA synthesized as described above was dispersed in 5 mL of $FeCl_3·6H_2O$ (10 mM), and the mixture was softly shaked for 1 min and then kept standing for 15 min. The obtained

DOI: 10.1021/acsami.5b03335
ACS Appl. Mater. Interfaces 2015, 7, 16338−16347

nanoparticles were collected by use of a magnet and washed with ethanol three times. Subsequently, the nanoparticles were redispersed in 5 mL of ethanolic solution containing H_3btc (10 mM), kept stewing for half an hour at 70 °C, separated by applying a magnet, and cleaned with enthanol three times. After repeating for 31 cycles, the as-synthesized nanoparticles were washed with ethanol and dried under vacuum at 150 °C.

2.3. Synthesis of Zr−MOF Nanoparticles. Zr−MOF nanoparticles were synthesized via a previous reported procedure.[38] Typically, 53 mg of $ZrCl_4$ and 38 mg of 1,4-benzenedicarboxylic acid (BDC) were resolved in 10 mL of *N*,*N*-dimethylformamide (DMF) for a solvothermal reaction in a Teflon-lined stainless steel autoclave at 120 °C for 24 h. Subsequently, 30 mg of as-synthesized Zr-MOF was dispersed in about 10 mL of chloroform for 5 days. Finally, the solid sample was extracted by filtration and dried under vacuum at 190 °C for 48 h.

2.4. Preparation of Tryptic Digests of Standard Proteins. First, 1 mg of β-casein and α-casein each were dissolved in 1 mL of ammonium bicarbonate solution (50 mM, pH = 8.2), respectively, and digested at 37 °C for 16 h with the addition of 40 μg of trypsin. Then, 1 mg of BSA was dissolved in 400 μL of 100 mmol L^{-1} NH_4HCO_3 and 8 mol L^{-1} urea (pH = 8.2) buffer, respectively. To reduce the disulfide bonds of the proteins, 10 μL of DTT (1 mmol L^{-1}) was added and the solution was maintained at 60 °C for 1 h. Then, 3.7 mg of IAA was added to the mixture to alkylate the protein in the dark place for about 40 min. Subsequently, the solution was diluted 10-fold with NH_4HCO_3 (50 mmol L^{-1}, pH = 8.2) and incubated with 40 μg of the trypsin at 37 °C for 16 h. Finally, the obtained tryptic digest was freeze-dried and preserved at −20 °C.

2.5. Pretreatment of Proteins Comes from Nonfat Milk. First, 30 μL of nonfat milk was diluted with 1 mL of NH_4HCO_3 (50 mM, pH = 8.2) and then centrifugated with a rotation speed of 16 000 rpm for 15 sec. The supernatant was saved, boiled at 100 °C for 10 min and then incubated for 16 h at 37 °C with an addition of 40 μg of trypsin.

2.6. Pretreatment of Human Serum. First, 2.5 μL of serum was added to 22.5 μL of loading buffer (ACN/H_2O/TFA, 60:39:1, v/v/v), softly blending for half an hour at 25 °C. The mixture was vortexed for a quarter min with a rotation speed of 1000 rpm, and then the supernatant was saved for further use.

2.7. Selective Enrichment of Phosphopeptides by Fe_3O_4@MIL-100 (Fe) Nanoparticles. First, 200 μg of the obtained Fe_3O_4@MIL-100 (Fe) nanoparticles were first washed with ethanol three times and then dispersed in 400 μL of loading buffer (ACN/H_2O/TFA, 60:39:1, v/v/v). Subsequently, tryptic digest of β-casein, α-casein was added into it respectively and incubated moderately at room temperature for 30 min. After that, the nanoparticles with the captured peptides were separated from the mixed solution with the help of a magnet and cleaned with 400 μL of the loading buffer three times to eliminate the nonspecifically adsorbed interferences. The trapped phosphopeptides were eluted with the eluting buffer $NH_3\cdot H_2O$ (2 × 10 μL, 10 wt %) and directly analyzed by MALDI-TOF MS. For comparison, original Fe_3O_4 nanoparticles and Zr-MOF nanoparticles were also used to selectively enrich phosphopeptides under the same enrichment conditions as those of Fe_3O_4@MIL-100 (Fe).

For phosphopeptides enrichment from complex sample, 300 μg of Fe_3O_4@MIL-100 (Fe) was mixed with tryptic digests of proteins prepared from nonfat milk and the human serum sample in 450 μL of loading buffer (ACN/H_2O/TFA, 60:39:1, v/v/v). The mixture was hatched at 25 °C for 40 min. After being cleaned by the loading buffer to eliminate the nonspecifically adsorbed interferences, the trapped phosphopeptides were eluted with the eluting buffer $NH_3\cdot H_2O$ (3 × 10 μL, 10 wt %). Finally, the eluent was kept for direct MALDI-TOF MS analysis.

2.8. Phosphopeptide Enrichment Recovery Test. According to a previously reported procedure, we divided a certain quantity of the standard phosphopeptide (LRRApSLGGK) equally into two parts and labeled with light and heavy isotopes according to a stable isotope dimethyl labeling approach.[39] Then, the heavy-tagged digest was treated with Fe_3O_4@MIL-100 (Fe) following the above-mentioned enrichment procedure. The resulting eluent was fully blended with the same quantity of the phosphopeptide of the light label, and the mixture was analyzed by MALDI-TOF MS. The enrichment recovery of the standard phosphopeptide was calculated by dividing the MS intensity ratio of phosphopeptide with the heavy label to that of light one.

2.9. Size-Exclusion Test of Fe_3O_4@MIL-100 (Fe) Core−Shell Magnetic Nanoparticles. To examine the size-exclusion effect of Fe_3O_4@MIL-100 (Fe) nanospheres, we mixed β-casein tryptic digest with BSA protein in 400 μL of the loading solution, then we put 200 mg of the Fe_3O_4@MIL-100 (Fe) into the solution. The mixture was incubated at 25 °C for 30 min. After the supernatant was removed, the nanoparticles collected by a magnet was cleaned with the loading buffer for three times and the captured peptides were regained by eluting with $NH_3\cdot H_2O$ (2 × 10 μL, 10 wt %).

2.10. MALDI-TOF MS Analysis. All the MALDI-TOF MS data were obtained from AB Sciex 5800 MALDI-TOF/TOF mass spectrometer (AB Sciex, CA) in a reflector positive mode with a pulsed Nd/YAG laser at 355 nm. For the detection of the phosphopeptides, acetonitrile aqueous solution (70%, v/v) containing DHB (25 mg/mL) and H_3PO_4 (1%, v/v) was prepared as a matrix. To test the protein sample, we employed the matrix SA (5 mg/mL). Then, 0.5 μL of the eluate and 0.5 μL of the corresponding matrix were dripped onto the MALDI plate in turn for MS analysis.

3. RESULTS AND DISCUSSION

3.1. Fabrication and Characterization of Fe_3O_4@MIL-100 (Fe) Nanoparticles. The synthesis process of the Fe_3O_4@MIL-100 (Fe) nanoparticle with Fe_3O_4 as the magnetic core, benzene-1,3,5-tricarboxylic acid (H_3btc) as the organic building blocks, Fe^{3+} as the metal precursor is illustrated in Scheme 1a. Briefly, Fe_3O_4 nanoparticle was prepared by solvothermal reaction with minor modification and then embellished with a monolayer of mercaptoacetic acid (MAA) to obtain Fe_3O_4-MAA. Subsequently, Fe_3O_4@MIL-100 (Fe) nanosphere was prepared via an alternative layer-by-layer assembly method with the modification of $FeCl_3$ and benzene-1,3,5-tricarboxylic acid (H_3btc) by turns. The layer-by-layer assembly approach introduced here is to form highly uniform coating of MOF layers on the Fe_3O_4 cores, which shows a great deal of merits such as convenience, low operating costs, especially accurate structure control, and a large number of binding sites of Fe_3O_4@MIL-100 (Fe). For comparison, the

Scheme 1. (a) Schematic Illustration of the Synthetic Procedure for the Preparation of Fe_3O_4@MIL-100 (Fe) Nanoparticles and (b) The Typical Process for Selective Enrichment of Phosphorylated Peptides Using Fe_3O_4@MIL-100 (Fe) Nanoparticles and Magnetic Separation

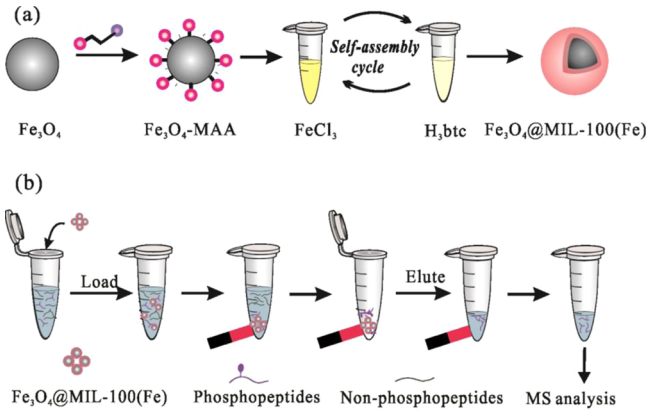

DOI: 10.1021/acsami.5b03335
ACS Appl. Mater. Interfaces 2015, 7, 16338−16347

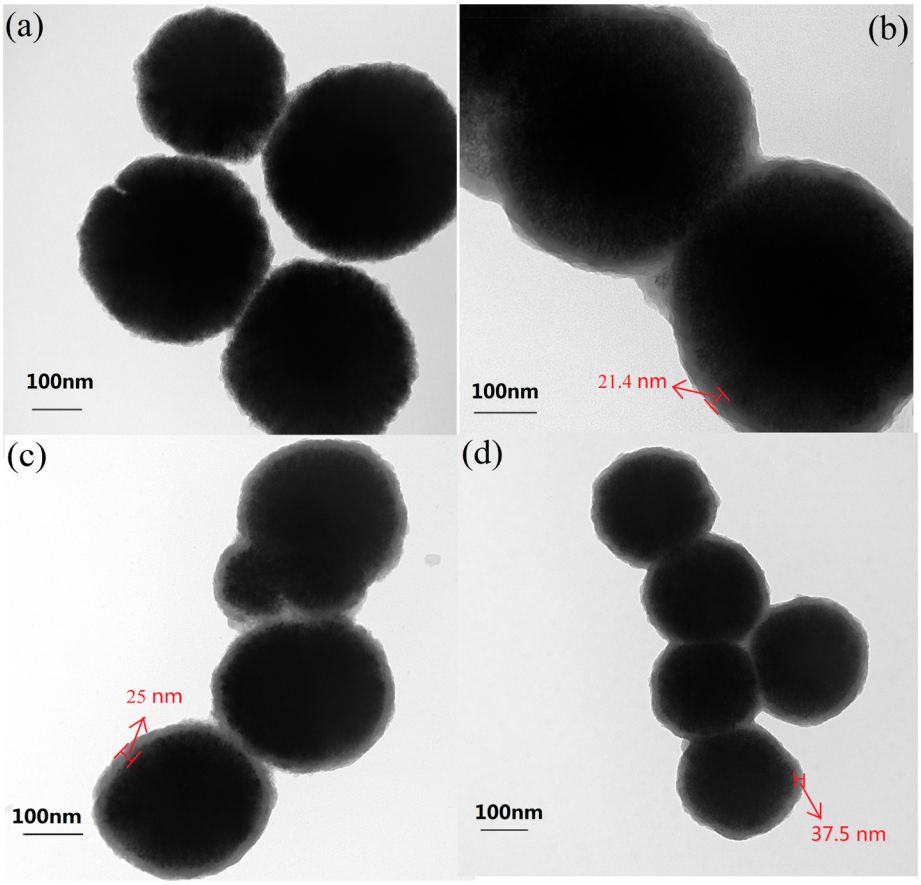

Figure 1. (a) TEM images of Fe_3O_4 cores. TEM images of core−shell magnetic nanoparticles of Fe_3O_4@MIL-100 (Fe) with (b) 21, (c) 31, and (d) 41 assembly cycles.

bare Fe_3O_4 nanoparticles and Zr−MOF were also synthesized for the following test.

Representative transmission electron microscopy (TEM) images of Fe_3O_4 and Fe_3O_4@MIL-100 (Fe) nanoparticles with different number of assembly cycles are shown in Figure 1. The Fe_3O_4 nanoparticles are uniform with no conglomeration and have a mean diameter of ca. 345 nm (Figure 1a). After being encapsuled with the MOF layer, the obtained Fe_3O_4@MIL-100 (Fe) nanospheres presented a neat core−shell structure and showed an obvious size increase. As can be seen from Figure 1b−d, the particle size of the nanospheres prepared increases gradually when the assembly cycle number grows (n = 21, 31, 41), with the MOF shell thickness of 21.4, 25, and 37.5 nm, respectively. And the obvious size increase suggests that the thickness of the MOF shell can be excellently regulated by altering the assembly cycle number taking advantage of the step-by-step assembly approach.

The modification of Fe_3O_4 particles with mercaptoacetic acid (MAA) before the assembly process is essential for the next stage of the step-by-step decoration. A MOF layer was tried to be directly wrapped onto the Fe_3O_4 surface without any modification. However, no expected resulting product was obtained. It is inferred that the carboxylate groups on the Fe_3O_4 particles are the initiators to the growth of the MOFs, which tightly bind a large sum of Fe^{3+} for the first layer, and then the btc units could be bound with the following reaction continues smoothly. Besides, the uniform growth of MOFs on the curved surface is usually undesirable. Randomly mixing MOF precursors and bare magnetic nanoparticles only led to autoagglutination of MOFs and nonuniformity, instability of final products, and surface modified with the carboxyl group could help to get well-organized growth of MOFs on the surface of the nanoparticles. Taking all these factors into consideration, the MAA layer was finally introduced to get the carboxylate-terminated magnetic cores.

To further prove the successful coating of the MOF layer, FT-IR spectroscopy was carried out to check the chemical structure of Fe_3O_4, Fe_3O_4@MIL-100 (Fe). As can be seen from Figure 2a, in comparison with the FT-IR spectrum of Fe_3O_4 (580 cm^{-1}, $\nu_{Fe-O-Fe}$), a new peak appears at 1715 nm^{-1}, which belongs to the stretching vibration of C═O in carboxyl groups. And the absorption peak at 1375 cm^{-1} ascribed to the C−O stretching vibration is also enhanced, demonstrating the appearance of carboxyl groups as well. In addition, the new characteristic peaks in the spectrum at 1566 and 1450 cm^{-1} belong to the stretching vibration of aromatic rings,[40] which indicates that the organic ligand H_3btc has been modified to the magnetic nanoparticles. All the evidence proves that the MOFs have been successfully decorated on the surface of the magnetic cores.

To study the porous structure of the Fe_3O_4@MIL-100 (Fe) nanoparticles, we also carried out nitrogen adsorption/desorption isotherms. As shown in Figure 2b, the nitrogen adsorption−desorption isotherms of Fe_3O_4@MIL-100 (Fe) nanoparticles show representative IV isotherm patterns of the porous material with a unique H4 hysteresis loop. An obvious capillary condensation step emerges between 0.4 and 0.6 P/P_0, also revealing that the material owns a microporous structure.

DOI: 10.1021/acsami.5b03335
ACS Appl. Mater. Interfaces 2015, 7, 16338−16347

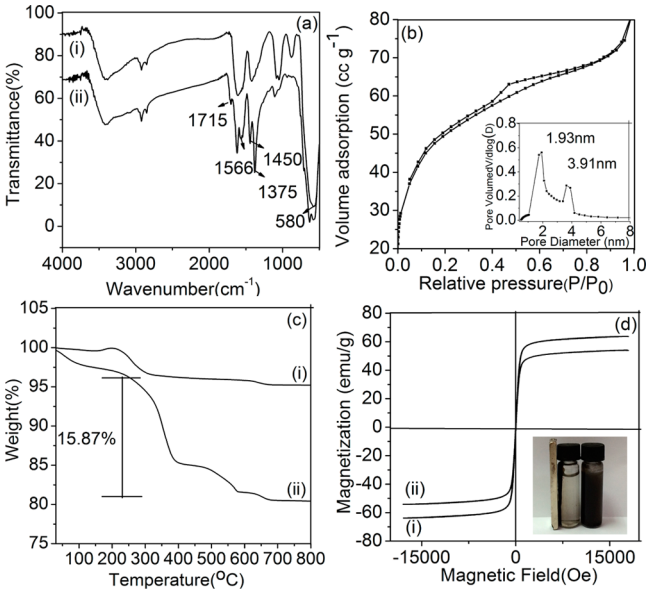

Figure 2. (a) FT-IR spectra of (i) Fe_3O_4, (ii) Fe_3O_4@MIL-100 (Fe); (b) N_2 adsorption/desorption isotherm of as-prepared Fe_3O_4@MIL-100 (Fe) measured at 77 K. The inset shows the pore size distribution obtained by DFT; (c) TGA curves and (d) Magnetization hysteresis loops of (i) Fe_3O_4 (ii) Fe_3O_4@MIL-100 (Fe).

The nitrogen adsorption abiding by the Brunauer–Emmett–Teller (BET) analysis was also carried out to test the surface area of the material, which is calculated to be 168.66 $m^2\ g^{-1}$. Besides, on the basis of the Barrett–Joyner–Halenda (BJH) model, the pore volume is calculated to be 0.13 $m^3\ g^{-1}$. Both values are lower than the MOF materials reported before via solvent thermal method because of the presence of the Fe_3O_4 cores. What's more, the pore size distribution of the core–shell nanoparticles (Figure 2b inset) shows two maxima at 1.93 and 3.91 nm, also revealing the porous structure of Fe_3O_4@MIL-100 (Fe) nanoparticles.

Thermogravimetric analysis (TGA) was recorded to prove the introduction of MOFs as well. The TGA curves (Figure 2c) show that the weight loss of 3.6% of Fe_3O_4 is attributed to the adsorbed water. And the weight loss of the MOFs decorated on the surface of Fe_3O_4 cores is calculated to be 15.87%, further demonstrating the presence of MOFs on the magnetic nanoparticles. The value is relatively low because of the thin thickness of the MOF shell, which can be controlled by varying the assembly cycles as mentioned above.

The magnetic characters of these two nanoparticles were investigated using a vibrating sample magnetometer at 25 °C (Figure 2d). The magnetic hysteresis curves of these two materials show no obvious remanence or coercivity at 25 °C, suggesting both of them all possess superparamagnetic feature. The superparamagnetism originates from the small clusters in the Fe_3O_4 nanospheres, which act as superparamagnets. And the saturation magnetization (Ms) value of them was measured to be 63.7 emu g^{-1}. After the coating of the MOF shell, the Ms value of the nanoparticles was tested as well, which arrived at 53.1 emu g^{-1}. Besides, compared to the bare Fe_3O_4 cores, Fe_3O_4@MIL-100 (Fe) nanoparticles were found to have better dispersibility and stability in water when there was no extrinsic magnetic force. Nevertheless, thanks to the high-magnetic response of Fe_3O_4 cores, the final product of Fe_3O_4@MIL-100 (Fe) nanoparticles could achieve quick separation less than half an hour utilizing a magnet (Figure 2d inset).

3.2. Selective Enrichment of Phosphopeptides from the Tryptic Digest of Standard Phosphoproteins. It is well-known that IMAC materials can be used as adsorbents for phosphopeptides, for example, immobilized Fe^{3+} or Zr^{4+} affinity chromatographic material has been reported to triumphantly enrich phosphopeptides from complex biological samples.[16,41,42] Therefore, to investigate the applicability of Fe_3O_4@MIL-100 (Fe) in the selective enrichment of phosphopeptides, we employed tryptic digest of a standard phosphoprotein (β-casein) to evaluate its performance. The enrichment flow is exhibited in Scheme 1b. First, β-casein digest was softly incubated with Fe_3O_4@MIL-100 (Fe). Then, after the separation of the nanoparticles from the mixture using a magnet and lavation with the fresh loading buffer, the trapped phosphopeptides were eluted and prepared for the MALDI-TOF MS analysis. As can be seen from Figure 3a, without the enrichment procedure, merely one phosphopetide was detected with poor MS intensity, low signal-to-noise ratio (S/N) and others were severely suppressed by large amount of non-phosphopeptides. However, after being treated by Fe_3O_4@MIL-100 (Fe), the signals of nonphosphopeptides were eliminated and three phosphopeptides along with their dephosphorylated counterparts (derived from the MALDI ionization process) were detected with high S/N ratio (Figure 3b).The minute description of the enriched phosphopeptides from tryptic digest of β-casein is presented in Table S-1 (SI). For comparison, Zr-MOF was also used to capture the phosphopeptides. However, only two of the targeted phosphopeptides can be identified with a much lower intensity (Figure 3c). In addition, the tryptic digest of β-casein was also enriched by Fe_3O_4, and the expected peaks representing the phosphopeptide with much worse signal intensity and S/N ratio were observed (Figure 3d). The enrichment efficiency of Fe_3O_4@MIL-100 (Fe) was evidently superior to that of Fe_3O_4 and Zr-metal organic framework, which can be attributed to the thick layer of MOFs on the material and the powerful chelating force among the Fe^{3+} ions and phosphate groups of

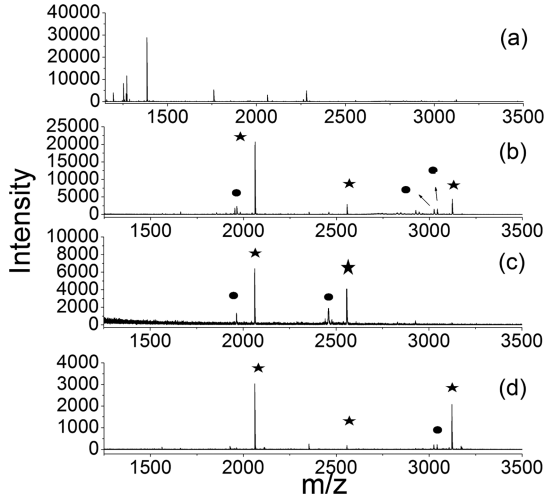

Figure 3. MALDI-TOF mass spectra of the tryptic digest of β-casein (0.5 pmol). (a) Direct analysis, after enrichment by (b) Fe_3O_4@MIL-100 (Fe) and (c) Zr-mental organic framework nanoparticles (d) Fe_3O_4 nanoparticles; (★) phosphopeptides and (●) dephosphorylated peptides.

DOI: 10.1021/acsami.5b03335
ACS Appl. Mater. Interfaces 2015, 7, 16338–16347

phosphopeptides. However, the local structure around the Fe^{3+} ions is difficult to determine. It is inferred that the Fe^{3+} ions exist in the MIL-100 with two structures. One is the $Fe_3O(CO_2)_6(OH)$ cluster, and the other is numerous Fe (III) carboxylate coordination polymers.[43,44] The Fe^{3+} ions in this cluster combine with a labile solvent atmosphere, forming a desirable interaction site for phosphate. These results reveal the excellent enrichment specificity of the Fe_3O_4@MIL-100 (Fe) nanoparticle for phosphopeptides.

To further evaluate the universal enrichment ability of the nanoparticles toward other phosphopeptides, we also used α-casein as the testing sample. As the testing results in Figure 4

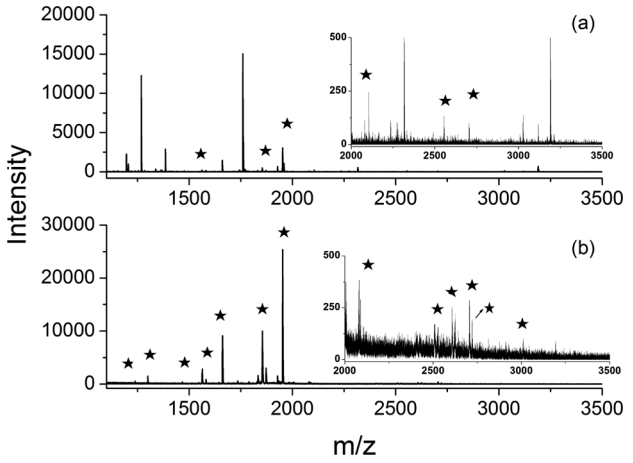

Figure 4. MALDI-TOF MS spectra of (a) direct analysis of 0.5 pmol tryptic digest of α-casein, (b) after enrichment by Fe_3O_4@MIL-100 (Fe); (★) phosphopeptides.

indicate, only several phosphopeptide MS peaks were observed through direct MS detection due to the serious signal suppression of the nonphosphorylated peptide MS peaks which dominated the MS spectrum with high intensities (Figure 4a). However, after being enriched by the Fe_3O_4@MIL-100 (Fe) nanoparticles, 16 expected phosphopeptides were easily detected with greatly improved S/N ratio and high peak intensity (Figure 4b). The explicit information on the trapped phosphopeptides from α-casein can be seen in Table S-2 (SI). All the results illustrate the good performance and excellent selectivity of Fe_3O_4@MIL-100 (Fe) for universal phosphopeptides enrichment.

It is well-known that the MOFs nanosphere has a unique pore structure, which can contribute to excluding the high molecular weight proteins and selectively extracting the peptides. To explore the size-exclusion effect of Fe_3O_4@MIL-100 (Fe), BSA was chosen as a high molecular weight interference to mix with the β-casein tryptic digest as a mimic sample due to its similarities with the main proteins of high concentrations in serum such as human serum albumin.[45] As shown in Figure 5a,b, because of the high-abundance protein and high-level salt existing in the mimic system, the MS intensities of phosphopeptides were severely suppressed and only three expected peaks of the BSA were observed around m/z of 15 000, 32 000, 68 000 respectively. Nevertheless, after enrichment by Fe_3O_4@MIL-100 (Fe), three expected peaks of the phosphopeptides as well as their dephosphorylate counterparts were clearly detected (Figure 5c), and no signal of BSA appeared in the MS spectrum any more (Figure 5d). The concentration of the BSA before and after enrichment in the

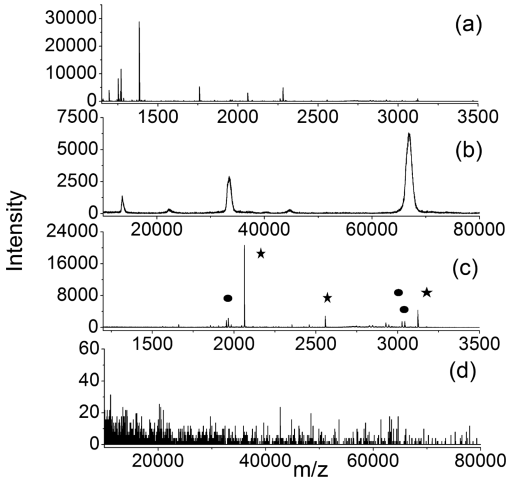

Figure 5. MALDI-TOF MS spectra of (a and c) 0.5 pmol β-casein and (b and d) 2.5 g L^{-1} BSA protein mixture: (a and b) without enrichment, and (c and d) after enrichment by Fe_3O_4@MIL-100 (Fe); (★) phosphopeptides and (●) dephosphorylated peptides.

loading buffer was detected by the Bradford method, which is calculated to be 0.033 and 0.030 mg mL^{-1}, respectively. There is only a little change of the concentration due to the unspecific adsorption, showing that the BSA was successfully excluded. We infer the reason is that the pore size is between the three-dimensional size of BSA and peptides, which could prevent the BSA proteins from entering it. In contrast, peptides whose sizes are smaller than the pore size will be permitted to enter the pores of the material easily. The result demonstrates that Fe_3O_4@MIL-100 (Fe) magnetic nanoparticles can efficaciously exclude high molecular weight proteins and enrich low molecular weight phosphopeptides.

To further evaluate the selectivity of the nanoparticles for phosphopeptides under the interference of other peptides, different amounts of tryptic digest of BSA were mixed with the tryptic digest of β-casein to construct an imitative biological sample. When the molar ratio of β-casein and BSA was 1:100, because of the serious signal suppression of the non-phosphorylated peptide peaks existing in the MS spectrum with high intensities (Figure 6a), nearly no phosphopeptide MS peak was observed through direct MS detection. However, after enrichment with Fe_3O_4@MIL-100 (Fe) nanoparticles, the S/N ratio of phosphopeptides was significantly improved, and the target phosphopeptides were identified with a clean background in the mass spectrum (Figure 6b). Although the molar ratio of β-casein and BSA was as low as 1:500, the target phosphopeptides still can be obviously detected with strong intensities (Figure 6c). The selectivity of the Fe_3O_4@MIL-100 (Fe) nanoparticles was better than the previously reported IMAC and IMOA magnetic microspheres, such us PA-Fe_3O_4@YPO_4 (1:300),[46] Fe_3O_4@Ti-mSiO_2 (1:100),[47] and (ZrP)-functionalized Fe_3O_4@mSiO_2 (1:50).[48] The high selectivity could be attributed to the pure carboxylic-Fe^{3+} surface and high concentration of the Fe^{3+} ions. The results show that the Fe_3O_4@MIL-100 (Fe) nanoparticles can selectively fish the phosphopeptides from complex mixtures.

3.3. Detection of the Binding Capacity, Enrichment Recovery, Detection Limit, Reusability and Batch-to-Batch Repeatability of Fe_3O_4@MIL-100 (Fe) in Phosphopeptides Enrichment. As the amount of phosphopeptides in a real complex biological sample is at the trace level, the

DOI: 10.1021/acsami.5b03335
ACS Appl. Mater. Interfaces 2015, 7, 16338−16347

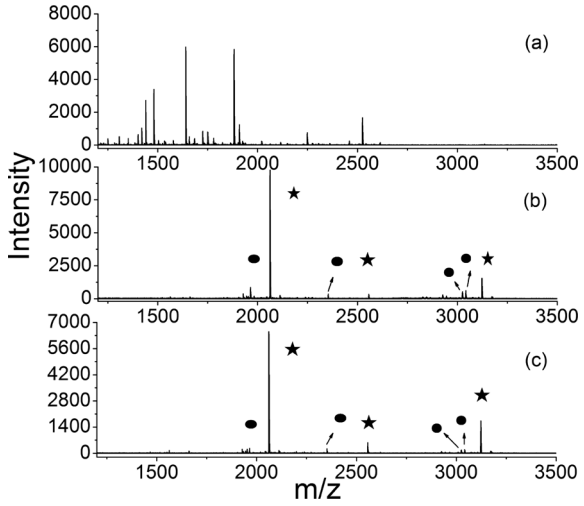

Figure 6. MALDI-TOF mass spectra of the tryptic digest mixture of β-casein (0.5 pmol) and BSA. (a) Direct analysis of the peptide mixture at a molar ratio of 1:100; after enrichment by Fe_3O_4@MIL-100 (Fe) nanoparticles at molar ratios of (b) 1:100, (c) 1:500; (★) phosphopeptides and (●) dephosphorylated peptides.

detection limit of Fe_3O_4@MIL-100 (Fe) toward phosphopeptides was investigated. Different amount of tryptic β-casein digest was treated with the prepared nanoparticles. As can be seen from Figure S-1a (SI), three targeted peaks could be clearly detected with the highest S/N ratios of 683.67 when 50 fmol of the tryptic β-casein digest was enriched by Fe_3O_4@MIL-100 (Fe) nanoparticles. Even when the total sum of β-casein tryptic digest was reduced to 0.5 fmol (Figure S-1c, SI), one targeted phosphopeptide of 3122.27 (m/z) could still be detected at a S/N ratio of 24.26. The obtained detection limit was superior to those of many IMAC and MOAC nanomaterials reported previously, for example, Fe_3O_4@mTiO_2 (10 fmol),[49] Fe_3O_4@PD-Ti^{4+} (2 fmol),[50] and mesoporous g-Fe_2O_3 (50 fmol).[51] Besides, the detection limit of the Zr−MOF was also tested. It can be seen from Figure S-1e (SI), only one weak peak with S/N ratio of 17.09 could be detected, which was quite inferior to the performance of Fe_3O_4@MIL-100 (Fe) under the same condition. And when the amount of β-casein tryptic digest was decreased to 0.5 pmol, no phosphopeptide peak appeared in the spectrum (Figure S-1f, SI). The high detection sensitivity of the Fe_3O_4@MIL-100 (Fe) nanoparticles may be ascribed to the large amount of immobilized Fe^{3+} ions, strong chelating force and unique magnetic responsibility of the Fe_3O_4@MIL-100 (Fe) nanoparticles. This result indicates that the detection limit of the prepared Fe_3O_4@MIL-100 (Fe) nanoparticles was at the fmol level for phosphopeptides.

To investigate the binding capacity of Fe_3O_4@MIL-100(Fe) as well as the Fe_3O_4 nanoparticles toward phosphopeptides, different quantities of Fe_3O_4@MIL-100(Fe) (5−100 μg) were used to enrich the same amount of β-casein tryptic digest (1.5 μg). Then 0.5 μL of the eluting fractions were analyzed via MALDI-TOF MS. When the intensity of one selected phosphopeptide (m/z = 2061.83) arrived at the maximum, the nanoparticls were saturated for the β-casein tryptic digest. As shown in Figure S-2a (SI), the binding capacity of the Fe_3O_4@MIL-100 (Fe) was calculated to be 60 mg g^{-1} which is much higher than that of the Fe_3O_4 particles (30 mg g^{-1}). The results reveal that the high density of the Fe^{3+} on the MOFs and powerful chelating force greatly improves the binding capacity of the prepared Fe_3O_4@MIL-100 (Fe) toward phosphopeptides. In addition, compared to the Fe_3O_4 nanoparticles, thanks to the size-exclusion effect of the MOF layer, the interference of some certain impurities are eliminated, which greatly improves the binding capacity of the Fe_3O_4@MIL-100 (Fe) nanoparticles.

To evaluate the enrichment recovery of the Fe_3O_4@MIL-100 (Fe) nanoparticles toward phosphopetides, the quantitative approach of stable isotope dimethyl labeling was introduced. Briefly, the same amount of β-casein (1 μg) tryptic digest was labeled with light and heavy isotopes. And then the heavy-isotope-tagged digest was treated with Fe_3O_4@MIL-100 (Fe) abiding by the above-mentioned enrichment. The eluate was mixed with the light labeled part and analyzed by MALDI-TOF MS. The enrichment recovery was calculated by the signal intensity of heavy-isotope-labeled phosphopeptide divided by light-isotope-labeled phosphopeptide. As the MALDI mass spectrum in Figure S-2b (SI) shows, the recovery of phosphopeptides from the Fe_3O_4@MIL-100 (Fe) nanoparticles was as high as 84.47%. It makes us believe that the Fe_3O_4@MIL-100 (Fe) nanoparticles can be an ideal magnetic IMAC adsorbent for phosphopeptides with extremely high enrichment recovery.

To investigate whether the Fe_3O_4@MIL-100 (Fe) nanoparticles can be recycled, the materials were regenerated by washing with the buffer solution three times. The regenerated Fe_3O_4@MIL-100 (Fe) nanoparticles were reused to enrich phosphopeptides from 0.5 pmol β-casein digest. As the MS detection results in Figure S-3 (SI) shows, even after being reused five times, the affinity probe still can efficiently capture the three targeted phosphopeptides with no sharp peak height decrease. This result indicates that our IMAC material can be recycled and reused for phosphopeptides enrichment. And we can infer that the Fe_3O_4@MIL-100 (Fe) nanoparticles synthesized via the layer-by-layer method are stable.

In addition, the batch-to-batch repeatability of the material was also tested. Three batches of the Fe_3O_4@MIL-100 (Fe) nanoparticles were synthesized at different times. Each was applied into the enrichment of digests of β-casein (0.5pmol) and α-casein (0.5 pmol) enrichment under the same experimental conditions. Although it is hard to quantify the phosphopeptides in the MS spectra, the peak height of 1953.02 (m/z) in the α-casein digest and 2061.57 (m/z) in the β-casein digest were chosen to indicate the repeatability of the material. The peak heights of the selected phosphopeptide peaks were shown in Table S-3 (SI), and the RSDs were calculated to be 3.34 and 3.93% respectively. The results show that the batch-to-batch repeatability of the Fe_3O_4@MIL-100 (Fe) nanoparticles is excellent due to the stability of the material and the strong cheating force between the Fe^{3+} and the phosphopeptides.

3.4. Highly Specific Enrichment of Phosphopeptides from Nonfat Milk and Human Serum. Inspired by the outstanding enrichment efficiency for standard phosphoprotein tryptic digest, nonfat milk was used to further investigate the enrichment performance of Fe_3O_4@MIL-100 (Fe) toward a real complex sample. For the tryptic digests of nonfat milk, as shown in Figure 7a, nonphosphopeptides dominated the spectrum so that nearly no phosphopeptide peaks appeared in the spectrum. Fortunately, after enrichment with the Fe_3O_4@MIL-100 (Fe) nanoparticles, 14 peaks of phosphopeptides distinctly appeared in the spectrum with a clean background (Figure 7b). In addition, we also choose the human serum as the testing sample, because it is a real complex sample mainly made up of high-abundance proteins (e.g.,

DOI: 10.1021/acsami.5b03335
ACS Appl. Mater. Interfaces 2015, 7, 16338−16347

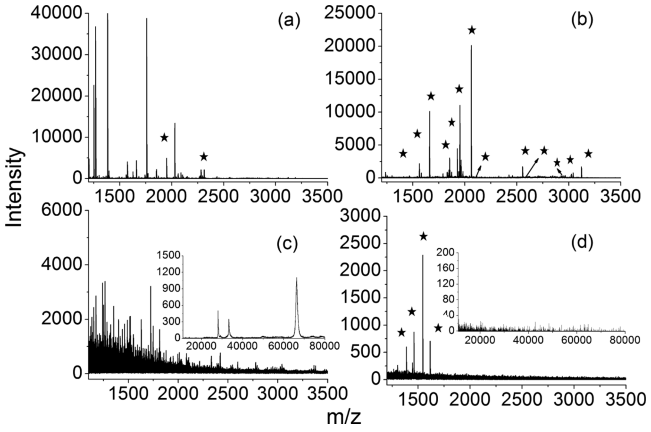

Figure 7. (a and (b) MALDI-TOF mass spectra of the tryptic digests of the milk before and after enrichment by Fe_3O_4@MIL-100 (Fe), respectively. (c and d) MALDI-TOF spectrum of human serum after enrichment by Fe_3O_4@MIL-100 (Fe), respectively; (★) phosphorylated peptides.

albumin, immunoglobulins) and a lesser amount of endogenous peptides.[52] The detection of low-abundance peptides is always tough due to the interference from high-abundance proteins. Thus, diluted healthy human serum was employed so as to further confirm the enrichment efficiency and the cutoff effectiveness of the Fe_3O_4@MIL-100 (Fe) nanoparticles. Figure 7c displays the direct analysis of peptides and proteins from human serum (Peptides mass range, 1000−3500 Da; proteins mass range, 10−80 kDa). Without treatment, nearly no peaks of the phosphopeptide and three peaks of high-abundance proteins, such as HSA appeared at m/z of 67 kDa were detected (Figure 7c). After treatment with the Fe_3O_4@MIL-100 (Fe) nanopaticles, the proteins of high molecular weight vanished (Figure 7d inset) and four endogenous phosphopeptides could be easily separated from the extremely complex biological system. It confirms that the 1.93 and 3.91 nm pores have a desirable cutoff effect to exclude most human serum proteins.[53] In comparison, the serum from an endometrial cancer patient was also enriched by Fe_3O_4@MIL-100 (Fe). The endogenous phosphopeptides can also be captured by the synthesized material without clear distinctions (Figure S-5, SI), which reveals that the Fe_3O_4@MIL-100 (Fe) nanoparticles could be successfully applied in the patient serum phosphopeptides enrichment and exclude the proteins as well. Besides, it can also be inferred from the same MS peaks that the endogenous phosphopeptides in the patient serum were not be influenced by the disease. The details of the detected phosphopeptides from the tryptic digests of nonfat milk and human serum are presented in Tables S-4 and S-5 (SI). The results suggest that the Fe_3O_4@MIL-100 (Fe) nanospheres have excellent size cutoff function for high molecular weight protein and ascendant enrichment selectivity for peptide from complex biological samples.

4. CONCLUSION

In summary, a novel porous IMAC material, Fe_3O_4@MIL-100 (Fe), with a uniform core−shell structure, super large surface area, nanopores of two pore sizes, rapid magnetic responsiveness, excellent structural stability was fabricated via a layer-by-layer assembly method. The modification of Fe_3O_4 particles with mercaptoacetic acid before the assembly process is crucial for the preparation of the target material. The investigation carried out to capture the phosphopeptides from mimic biological mixtures indicated that the Fe_3O_4@MIL-100 (Fe) nanoparticles had a high specificity, extremely low detection, large enrichment capacity, super high enrichment recovery, excellent reusability and batch-to-batch repeatability for the selective enrichment of phosphopeptides. Moreover, the Fe_3O_4@MIL-100 (Fe) nanoparticles show great practicability for selective enrichment of phosphopeptides from real biological samples, which is mainly due to their eximious water dispersibility, the abundant immobilized Fe (III) ions, and the strong chelating force among Fe (III) ions and phosphate groups of phosphopeptides. Additionally, it was manifested that the magnetic nanoparticles could selectively capture phosphopeptides from human serum (both the healthy and the unhealthy) and exclude the high molecular weight proteins in it at the same time. It is expected that the Fe_3O_4@MIL-100 (Fe) magnetic nanoparticles could be a useful tool for trapping of phosphopeptides from complex biological sample.

■ ASSOCIATED CONTENT

Supporting Information

Detailed information on the trapped phosphopeptides; characterization; mass spectra of the detection limit; the recovery, enrichment capacity, batch-to-batch repeatability, reusability of the material. The Supporting Information is available free of charge on the ACS Publications website at DOI: 10.1021/acsami.5b03335.

■ AUTHOR INFORMATION

Corresponding Author

* E-mail: weibingzhang@ecust.edu.cn. Tel: 86-21-64252145. Fax: 86-21-64233161.

Author Contributions

All authors have given approval to the final version of the manuscript.

Notes

The authors declare no competing financial interest.

■ ACKNOWLEDGMENTS

Financial support is gratefully acknowledged from Science Foundation for Young Scientists of China (No. 21105027), support of the National Natural Science Foundation of China (No.21475044), the Key Research Project from the Ministry of Public Security (201202ZDYJ005), the National Key Scientific Instrument and Equipment Development Project (2012YQ120044).

■ REFERENCES

(1) Ptacek, J.; Devgan, G.; Michaud, G.; Zhu, H.; Zhu, X. W.; Fasolo, J.; Guo, H.; Jona, G.; Breitkreutz, A.; Sopko, R.; McCartney, R. R.; Schmidt, M. C.; Rachidi, N.; Lee, S. J.; Mah, A. S.; Meng, L.; Stark, M. J. R.; Stern, D. F.; De Virgilio, C.; Tyers, M.; Andrews, B.; Gerstein, M.; Schweitzer, B.; Predki, P. F.; Snyder, M. Global Analysis of Protein Phosphorylation in Yeast. *Nature* **2005**, *438*, 679−684.

(2) Olsen, J. V.; Blagoev, B.; Gnad, F.; Macek, B.; Kumar, C.; Mortensen, P.; Mann, M. Global, In Vivo, and Site-Specific Phosphorylation Dynamics in Signaling Networks. *Cell* **2006**, *127*, 635−648.

(3) Zolnierowicz, S.; Bollen, M. Protein Phosphorylation and Protein Phosphatases De Panne, Belgium, September 19−24, 1999. *EMBO J.* **2000**, *19*, 483−488.

(4) Gronborg, M.; Kristiansen, T. Z.; Stensballe, A.; Andersen, J. S.; Ohara, O.; Mann, M.; Jensen, O. N.; Pandey, A. A Mass Spectrometry-

DOI: 10.1021/acsami.5b03335
ACS Appl. Mater. Interfaces 2015, 7, 16338−16347

based Proteomic Approach for Identification of Serine/Threonine-Phosphorylated Proteins by Enrichment with Phospho-Specific Antibodies- Identification of a Novel Protein, Frigg, as a Arotein Kinase A substrate. *Mol. Cell. Proteomics* **2002**, *1*, 517−527.
(5) Montoya, A.; Beltran, L.; Casado, P.; Rodriguez-Prados, J. C.; Cutillas, P. R. Characterization of a TiO_2 Enrichment Method for Label-Free Quantitative Phosphoproteomics. *Methods* **2011**, *54*, 370−378.
(6) Thingholm, T. E.; Jorgensen, T. J. D.; Jensen, O. N.; Larsen, M. R. :Highly Selective Enrichment of Phosphorylated Peptides Using Titanium Dioxide. *Nat. Protoc* **2006**, *1*, 1929−1935.
(7) Min, Q. H.; Zhang, X. X.; Zhang, H. Y.; Zhou, F.; Zhu, J. J. Synthesis of Fe_3O_4-Graphene-TiO_2 Ternary Composite Networks for Enhanced Capture of Phosphopeptides. *Chem. Commun.* **2011**, *47*, 11709−11711.
(8) Nuhse, T. S.; Stensballe, A.; Jensen, O. N.; Peck, S. C. Large-Scale Analysis of In Vivo Phosphorylated Membrane Proteins by Immobilized Metal Ion Affinity Chromatography and Mass Spectrometry. *Mol. Cell. Proteomics* **2003**, *2*, 1234−1243.
(9) Feng, S.; Ye, M. L.; Zhou, H. J.; Jiang, X. G.; Jiang, X. N.; Zou, H. F.; Gong, B. L. Immobilized Zirconium Ion Affinity Chromatography for Specific Enrichment of Phosphopeptides in Phosphoproteome Analysis. *Mol. Cell. Proteomics* **2007**, *6*, 1656−1665.
(10) Xiong, Z. C.; Zhang, L. Y.; Fang, C. L.; Zhang, Q. Q.; Ji, Y. S.; Zhang, Z.; Zhang, W. B.; Zou, H. F. Ti^{4+}-Immobilized Multilayer Polysaccharide Coated Magnetic Nanoparticles for Highly Selective Enrichment of Phosphopeptides. *J. Mater. Chem. B* **2014**, *2*, 4473−4480.
(11) Ma, W. F.; Zhang, Y.; Li, L. L.; Zhang, Y. T.; Yu, M.; Guo, J.; Lu, H. J.; Wang, C. C. : Ti^{4+}-Immobilized Magnetic Composite Microspheres for Highly Selective Enrichment of Phosphopeptides. *Adv. Funct. Mater.* **2013**, *23*, 107−115.
(12) Mohammed, S.; Heck, A. J. R. Strong Cation Exchange (SCX) Based Analytical Methods for the Targeted Analysis of Protein Post-Translational Modifications. *Curr. Opin. Biotechnol.* **2011**, *22*, 9−16.
(13) Dong, M. M.; Wu, M. H.; Wang, F. J.; Qin, H. Q.; Han, G. H.; Gong, J.; Wu, R. A.; Ye, M. L.; Liu, Z.; Zou, H. F. Coupling Strong Anion-Exchange Monolithic Capillary with MALDI-TOF MS for Sensitive Detection of Phosphopeptides in Protein Digest. *Anal. Chem.* **2010**, *82*, 2907−2915.
(14) Tan, F.; Zhang, Y. J.; Wei, Mi.; Wang, J. L.; Wei, J. Y.; Cai, Y.; Qian, X. H. Enrichment of Phosphopeptides by Fe^{3+}-Immobilized Magnetic Nanoparticles for Phosphoproteome Analysis of the Plasma Membrane of Mouse Liver. *J. Proteome. Res.* **2007**, *7*, 1078−1087.
(15) Feng, S.; Pan, C. S.; Jiang, X. G.; Xu, S. Y.; Zhou, H. J.; Ye, M. L.; Zou, H. F. Fe^{3+} Immobilized Metal Affinity Chromatography with Silica Monolithic Capillary Column for Phosphoproteome Analysis. *Proteomics* **2007**, *7*, 351−360.
(16) Pan, C. S.; Ye, M. L.; Liu, Y. G.; Feng, S.; Jiang, X. G.; Han, G. H.; Zhu, J. J.; Zou, H. F. Enrichment of Phosphopeptides by Fe^{3+}-Immobilized Mesoporous Nanoparticles of MCM-41 for MALDI and Nano-LC-MS/MS Analysis. *J. Proteome. Res.* **2006**, *5*, 3114−3124.
(17) Yan, Y. H.; Zhang, X. M.; Deng, C. H. Functionalized Magnetic Nanoparticles for Sample Preparation in Proteomics and Peptidomics Analysis. *Chem. Soc. Rev.* **2013**, *42*, 8517−8539.
(18) Zheng, J.; Li, Y. P.; Sun, Y. F.; Yang, Y. K.; Ding, Y.; Lin, Y.; Yang, W. L. : A Generic Magnetic Microsphere Platform with "Clickable" Ligands for Purification and Immobilization of Targeted Proteins. *ACS Appl. Mater. Interfaces* **2015**, *7*, 7241−7250.
(19) Sun, N.; Deng, C.; Li, Y.; Zhang, X. Size-Exclusive Magnetic Graphene/Mesoporous Silica Composites with Titanium(IV)-Immobilized Pore Walls for Selective Enrichment of Endogenous Phosphorylated Peptides. *ACS Appl. Mater. Interfaces* **2014**, *6*, 11799−11804.
(20) Wang, Z. G.; Cheng, G.; Liu, Y. L.; Zhang, J. L.; Sun, D. H.; Ni, J.. Z. Novel Core-Shell Cerium(IV)-Immobilized Magnetic Polymeric Microspheres for Selective Enrichment and Rapid Separation of Phosphopeptides. *J. Colloid Interface Sci.* **2014**, *417*, 217−226.
(21) Zhang, Y.; Ma, W. F.; Zhang, C.; Wang, C. C.; Lu, H. J. : Titania Composite Microspheres Endowed with a Size-Exclusive Effect toward the Highly Specific Revelation of Phosphopeptidome. *ACS Appl. Mater. Interfaces* **2014**, *6*, 6290−6299.
(22) Murray, L. J.; Dinca, M.; Long, J. R. Hydrogen Storage in Metal-Organic Frameworks. *Chem. Soc. Rev.* **2009**, *38*, 1294−1314.
(23) Chang, N.; Gu, Z. Y.; Yan, X. P. Zeolitic Imidazolate Framework-8 Nanocrystal Coated Capillary for Molecular Sieving of Branched Alkanes from Linear Alkanes along with High-Resolution Chromatographic Separation of Linear Alkanes. *J. Am. Chem. Soc.* **2010**, *132*, 13645−13647.
(24) Gu, Z. Y.; Yan, X. P. Metal−Organic Framework MIL-101 for High-Resolution Gas-Chromatographic Separation of Xylene Isomers and Ethylbenzene. *Angew. Chem., Int. Ed.* **2010**, *49*, 1477−1480.
(25) Gu, Z. Y.; Yang, C. X.; Chang, N.; Yan, X. P. Metal-Organic Frameworks for Analytical Chemistry: From Sample Collection to Chromatographic Separation. *Acc. Chem. Res.* **2012**, *45*, 734−745.
(26) Yang, C. X.; Yan, X. P. Metal−Organic Framework MIL-101(Cr) for High-Performance Liquid Chromatographic Separation of Substituted Aromatics. *Anal. Chem.* **2011**, *83*, 7144−7150.
(27) Kreno, L. E.; Leong, K.; Farha, O. K.; Allendorf, M.; Van Duyne, R. P.; Hupp, J. T. Metal-Organic Framework Materials as Chemical Sensors. *Chem. Rev.* **2012**, *112*, 1105−1125.
(28) Rojas, S.; Wheatley, P. S.; Quartapelle-Procopio, E.; Gil, B.; Marszalek, B.; Morris, R. E.; Barea, E. Metal-Organic Frameworks as Potential Multi-Carriers of Drugs. *CrystEngComm* **2013**, *15*, 9364−9367.
(29) Feng, D. W.; Liu, T. F.; Su, J.; Bosch, M.; Wei, Z. W.; Wan, W.; Yuan, D. Q.; Chen, Y. P.; Wang, X.; Wang, K. C.; Lian, X. Z.; Gu, Z. Y.; Park, J.; Zou, X. D.; Zhou, H. C. Stable Metal-Organic Frameworks Containing Single-Molecule Traps for Enzyme Encapsulation. *Nat. Commun.* **2015**, *6*, 5979.
(30) Saeed, A.; Maya, F.; Xiao, D. J.; Najam-ul-Haq, M.; Svec, F.; Britt, D. K. Growth of a Highly Porous Coordination Polymer on a Macroporous Polymer Monolith Support for Enhanced Immobilized Metal Ion Affinity Chromatographic Enrichment of Phosphopeptides. *Adv. Funct. Mater.* **2014**, *24*, 5790−5797.
(31) Liu, W. L.; Lo, S. H.; Singco, B.; Yang, C. C.; Huang, H. Y.; Lin, C. H. Novel Trypsin-FITC@MOF Bioreactor Efficiently Catalyzes Protein Digestion. *J. Mater. Chem. B* **2013**, *1*, 928−932.
(32) Zheng, J.; Lin, Z.; Lin, G.; Yang, H.; Zhang, L. Preparation of Magnetic Metal-Organic Framework Nanocomposites for Highly Specific Separation of Histidine-Rich Proteins. *J. Mater. Chem. B* **2015**, *3*, 2185−2191.
(33) Zhang, Y. W.; Li, Z.; Zhao, Q.; Zhou, Y. L.; Liu, H. W.; Zhang, X. X. A Facilely Synthesized Amino-Functionalized Metal-Organic Framework for Highly Specific and Efficient Enrichment of Glycopeptides. *Chem. Commun.* **2014**, *50*, 11504−11506.
(34) Gu, Z. Y.; Chen, Y. J.; Jiang, J. Q.; Yan, X. P. Metal-Organic Frameworks for Efficient Enrichment of Peptides with Simultaneous Exclusion of Proteins from Complex Biological Samples. *Chem. Commun.* **2011**, *47*, 4787−4789.
(35) Zhao, M.; Deng, C. M.; Zhang, X. M.; Yang, P. Y. : Facile Synthesis of Magnetic Metal-Organic Frameworks for the Enrichment of Low-Abundance Peptides for MALDI-TOF MS Analysis. *Proteomics* **2013**, *13*, 3387−3392.
(36) Xiong, Z. C.; Ji, Y. S.; Fang, C. L.; Zhang, Q. Q.; Zhang, L. Y.; Ye, M. L.; Zhang, W. B.; Zou, H. F. Facile Preparation of Core-Shell Magnetic Metal-Organic Framework Nanospheres for the Selective Enrichment of Endogenous Peptides. *Chem. - Eur. J.* **2014**, *20*, 7389−7395.
(37) Zhao, M.; Deng, C. H.; Zhang, X. M. The Design and Synthesis of a Hydrophilic Core-Shell-Shell Structured Magnetic Metal-Organic Framework as a Novel Immobilized Metal Ion Affinity Platform for Phosphoproteome Research. *Chem. Commun.* **2014**, *50*, 6228−6231.
(38) Abid, H. R.; Tian, H. Y.; Ha, M. A.; Moses, O. T.; Craig, E. B.; Wang, S. B. Nanosize Zr-metal Organic Framework (UiO-66) for Hydrogen and Carbon Dioxide Storage. *Chem. Eng. J.* **2012**, *187*, 415−420.

DOI: 10.1021/acsami.5b03335
ACS Appl. Mater. Interfaces 2015, 7, 16338−16347

(39) Boersema, P. J.; Raijmakers, R.; Lemeer, S.; Mohammed, S.; Heck, A. J. R. Multiplex Peptide Stable Isotope Dimethyl Labeling for Quantitative Proteomics. *Nat. Protoc.* **2009**, *4*, 484−494.
(40) Hu, Y. L.; Fan, Y. F.; Huang, Z. L.; Song, C. Y.; Li, G. K. In Situ Fabrication of Metal-Organic Hybrid Gels in a Capillary for Online Enrichment of Trace Analytes in Aqueous Samples. *Chem. Commun.* **2012**, *48*, 3966−3968.
(41) Huang, J.; Guo, L.; Zheng, L. M. Rapid Enrichment and Determination of Phosphopeptides Using Bacterial Magnetic Particles *via* Both Strong and Weak Interactions. *Analyst* **2010**, *135*, 559−563.
(42) Zhao, M.; Zhang, X. M.; Deng, C. H. Facile Synthesis of Hydrophilic Magnetic Graphene@Metal-Organic Framework for Highly Selective Enrichment of Phosphopeptides. *RSC Adv.* **2015**, *5*, 35361−35364.
(43) Gerard, F.; Christian, S.; Caroline, M. D.; Franck, M.; Suzy, S.; Julien, D.; Irene, M. A Hybrid Solid with Giant Pores Prepared by a Combination of Targeted Chemistry, Simulation, and Powder Diffraction. *Angew. Chem.* **2004**, *43*, 6456−6461.
(44) Horcajada, P.; Surble, S.; Serre, C.; Hong, D.-Y.; Seo, Y.-K.; Chang, J.-S.; Greneche, J.-M.; Margiolaki, I.; Ferey, G. Synthesis and Catalytic Properties of MIL-100(Fe), an Iron(III) Carboxylate with Large Pores. *Chem. Commun.* **2007**, 2820−2822.
(45) Schrader, M.; Schulz, K. P. Peptidomics Technologies for Human Body Fluids. *Trends Biotechnol.* **2001**, *19*, S55−S60.
(46) Sun, Y.; Wang, H. F. Ultrathin-Yttrium Phosphate-Shelled Polyacrylate-Ferriferrous Oxide Magnetic Microspheres for Rapid and Selective Enrichment of Phosphopeptides. *J. Chromatogr. A* **2013**, *1316*, 62−68.
(47) Li, X. S.; Pan, Y. N.; Zhao, Y.; Yuan, B. F.; Guo, L.; Feng, Y. Q. Preparation of Titanium-Grafted Magnetic Mesoporous Silica for the Enrichment of Endogenous Serum Phosphopeptides. *J. Chromatogr. A* **2013**, *1315*, 61−69.
(48) Lu, J.; Li, Y.; Deng, C. H. Facile Synthesis of Zirconium Phosphonate-Functionalized Magnetic Mesoporous Silica Microspheres Designed for Highly Selective Enrichment of Phosphopeptides. *Nanoscale* **2011**, *3*, 1225−1233.
(49) Ma, W. F.; Zhang, Y.; Li, L. L.; You, L. L.; Zhang, P.; Zhang, Y. T.; Li, J. M.; Yu, M.; Guo, J.; Lu, H. J.; Wang, C. C. Tailor-Made Magnetic Fe_3O_4@mTiO_2 Microspheres with a Tunable Mesoporous Anatase Shell for Highly Selective and Effective Enrichment of Phosphopeptides. *ACS Nano* **2012**, *6*, 3179−3188.
(50) Yan, Y. H.; Zheng, Z. F.; Deng, C. H.; Zhang, X. M.; Yang, P. Y. Facile Synthesis of Ti^{4+}-Immobilized Fe_3O_4@Polydopamine Core-Shell Microspheres for Highly Selective Enrichment of Phosphopeptides. *Chem. Commun.* **2013**, *49*, 5055−5057.
(51) Zhang, Y. T.; Li, L. L.; Ma, W. F.; Zhang, Y.; Yu, M.; Guo, J.; Lu, H. J.; Wang, C. C. Two-in-One Strategy for Effective Enrichment of Phosphopeptides Using Magnetic Mesoporous Gamma-Fe_2O_3 Nanocrystal Clusters. *ACS Appl. Mater. Interfaces* **2013**, *5*, 614−621.
(52) Tirumalai, R. S.; Chan, K. C.; Prieto, D. A.; Issaq, H. J.; Conrads, T. P.; Veenstra, T. D. Characterization of the Low Molecular Weight Human Serum Proteome. *Mol. Cell. Proteomics* **2003**, *2*, 1096−1103.
(53) Villanueva, J.; Philip, J.; Entenberg, D.; Chaparro, C. A.; Tanwar, M. K.; Holland, E. C.; Tempst, P. Serum Peptide Profiling by Magnetic Particle-Assisted, Automated Sample Processing and MALDI-TOF Mass Spectrometry. *Anal. Chem.* **2004**, *76*, 1560−1570.

DOI: 10.1021/acsami.5b03335
ACS Appl. Mater. Interfaces 2015, 7, 16338−16347